Available online at www.sciencedirect.com
ScienceDirect
Trans. Nonferrous Met. Soc. China 25(2015) 1559−1567
Transactions of Nonferrous Metals Society of China
www.tnmsc.cn

Preparation and characterization of ZnSe/CdSe core-shell microspheres

Yu-lu DUAN[1], Li-qi ZHOU[1], Guo-fu XU[1,2], Hui-ying ZHANG[1], Xu LI[1], Xiao-he LIU[1]

1. School of Materials Science and Engineering, Central South University, Changsha 410083, China;
2. Key Laboratory of Nonferrous Materials Science and Engineering, Ministry of Education, Central South University, Changsha 410083, China

Received 4 May 2014; accepted 29 July 2014

Abstract: The preparation of ZnSe/CdSe core-shell structure nanocomposites by using the re-prepared ZnSe microspheres as the template under the hydrothermal condition was presented. The influence of different mole ratios of ZnSe to $Cd(NO_3)_2$ on the morphology and structure of the final product was investigated. And the performances of ZnSe/CdSe core-shell structure nanocomposites were characterized by the means of X-ray diffraction (XRD) analyses, scanning electron microscopy (SEM), transmission electron microscopy (TEM) and photoluminescence (PL) spectroscopy. The results indicate that the core-shell structure product can be prepared, when the mole ratio of ZnSe to $Cd(NO_3)_2$ is larger than 1:1; and the product will be ball solid structure, when the mole ratio of ZnSe to $Cd(NO_3)_2$ is equal to 1:1. The photo luminescence results show that ZnSe/CdSe core-shell structures have high photo luminescence emission properties, and the product with mole ratio of ZnSe to $Cd(NO_3)_2$ being 1:0.5 has the best luminescence properties.

Key words: hydrothermal methed; core-shell nanocomposite; ZnSe; CdSe; optical property

1 Introduction

Synthesis of nanometer-sized particles of A(II)B(VI) (where A=Cd, Zn and B=S, Se, Te) semiconducting compounds has attracted a great deal of interests in recent years [1]. This is due to the fact that studies of such particles provide an opportunity to observe, fine tune and modify the relationship between physical properties, size and shape for a given chemical compound [2]. The II−VI semiconducting compounds ZnSe and CdSe have large direct band gaps and they are used for LED and display [3]. Furthermore, core-shell and hollow microspheres have attracted interest increasingly because of their potential applications in catalysis, delivery and controlled release, artificial cells, optoelectronics, microcavity resonance, and photonic crystals [4]. The stable efficient luminescence of the core-shell particles is superior to single phase nanoparticles, organic dyes and light-emitting devices [5]. For the visible spectral range, CdSe nanocrystals are considered the most promising emitting material because their emission color can be precisely adjusted from blue to red. In the case of ZnSe/CdSe core-shells, the lattice mismatch between the core and the shell materials is relatively small, which leads to a low concentration of defects in the shell. Meanwhile, the ZnSe/CdSe nanocrystals exhibit high photoluminescence (PL) quantum efficiencies, up to 80%−90% [6].

To date, many approaches have been suggested for the synthesis of groups II−VI semiconductor crystallites or nanocrystallines, such as various physical methods including hydrothermal process [7], chemical vapor deposition (CVD) [8−10], electrodeposition [11], and template−directed growth [12], and mechanochemical synthesis from Zn and Se granules. Generally, all these reactions require high temperature (500 °C) and the use of toxic and highly sensitive precursors. Recently, nanocrystalline ZnSe has been synthesized by different hydrothermal methods and derivatives thereof. JIAO et al [13] prepared ZnSe quantum dots (QD) hydrothermally using $ZnCl_2$ and Na_2SeO_3 as Zn and Se sources and hydrazine was used as the reducing agent. BANDARANAYKE et al [14] reported a method for synthesis of CdE(S, Se, Te) crystallites using aqueous solution precipitation from Na_2E(S, Se, Te) and $CdCl_2$ followed by thermal annealing at high temperature. However, this method still needs relatively high

Foundation item: Project (13JJ1005) supported by the Natural Science Foundation for Distinguished Young Scholars of Hunan Province, China
Corresponding author: Guo-fu XU; Tel: +86-731-88877217; E-mail: csuxgf66@csu.edu.cn
DOI: 10.1016/S1003-6326(15)63758-X

temperature or high pressure and long reaction time (several hours to days). However, the synthesis of ZnSe coated CdSe core-shell microspheres has not been reported. It is probably because of the high crystallinity of ZnSe and the weak interaction between ZnSe and CdSe [15].

In this work, we report a new approach to synthesize ZnSe/CdSe core-shell microspheres by a templated method based on the hydrothermal system. The templates used here are re-prepared ZnSe microspheres via hydrothermal method. Compared with that of the previously studied sonochemical method, the new method is much simpler, safer, and more general for the preparation of ZnSe/CdSe core-shell microspheres. Through a serials of comparing experiments, we believe that different mole ratios of ZnSe to $Cd(NO_3)_2$ have a decisive effect on the final ZnSe/CdSe core-shell microspheres morphology. The morphology and structure of the products were investigated while their room temperature photoluminescence (PL) properties were tested. Lastly, the synthesis mechanism of ZnSe/CdSe core-shell nanocomposites was revealed.

2 Experimental

All chemical solvent and reagents used in this work, such as aqueous zinc nitrate ($Zn(NO_3)_2{\cdot}6H_2O$), sodium selenite (Na_2SeO_3), sodium hydroxide (NaOH), hydrazine hydrate ($N_2H_4{\cdot}H_2O$) and cadmium nitrate tetrahydrate ($Cd(NO_3)_2{\cdot}4H_2O$), were of analytical grade and used without any further purification. Deionized water was used in all preparations.

2.1 Synthesis of ZnSe nanocrystals

In a typical procedure, 0.298 g $Zn(NO_3)_2{\cdot}6H_2O$ and 0.173 g Na_2SeO_3 were added into a 50 mL of Teflon-lined stainless steel autoclave and dissolved in 20 mL 1 mol/L NaOH solution through supersonic vibration. Then, 10 mL of hydrazine monohydrate (80%, volume fraction) solution was added dropwise during vigorous stirring. Next, 10 mL of deionized water was added into the autoclave that was filled up to 80% of the total volume. After 10 min stirring, the autoclave was sealed and maintained at 180 °C for 4 h. Subsequently, the system was allowed to cool to the room temperature naturally. The resulting precipitate was collected by centrifugal sedimentation, washed with absolute ethanol and distilled water in sequence for several times. The final product was dried at 60 °C for 8 h [16,17].

2.2 Synthesis of ZnSe/CdSe core-shell systems

The conversion from ZnSe to ZnSe/CdSe core-shell nanocrystals can be realized due to the much different solubility between them. The K_{sp} ($10^{-35.2}$) value of CdSe is lower than that of ZnSe ($10^{-29.4}$). To obtain microspheres of CdSe, high ionic concentrations and additional energy (by heating to 140 °C) are required to successfully complete the conversion reaction [17].

$$ZnSe + Cd^{2+} \overset{140\ ^\circ C}{\rightleftharpoons} CdSe + Zn^{2+} \quad (1)$$

0.144 g ZnSe and 0.077 g, 0.154 g, 0.231 g $Cd(NO_3)_2{\cdot}4H_2O$ were added into a 50 mL volume of Teflon-lined stainless steel autoclave and dissolved in 35 mL EDTA solution through supersonic vibration, respectively. The preparation method of EDTA is that 0.887 g ethylenediaminetetraacetic acid was dissolved in 40 mL 0.5 mol/L NaOH solution. Then 5 mL of hydrazine monohydrate (80%, volume fraction) solution was added dropwise during vigorous stirring. After 10 min stirring, the autoclave was sealed and maintained at 140 °C for 48 h. Subsequently, the system was allowed to cool to the room temperature naturally. The resulting precipitate was collected by centrifugal sedimentation, washed with absolute ethanol and distilled water in sequence for several times. The final product was dried at 60 °C for 8 h.

2.3 Characterization of materials

The obtained products were characterized with a Rigaku D/MAX2500 X-ray diffractometer (XRD) with Cu K_α radiation (λ=0.154051 nm). The operation voltage and current were kept at 40 kV and 40 mA, respectively. The size and morphology of the as-synthesized products were determined at 10 kV by a Sirion 200 field emission scanning electron microscope (SEM) and at 200 kV by a Tecnai G2 20ST transmission electron microscope (TEM) and a JEOL JEM−2100F high-resolution transmission electron microscope (HRTEM). Energy-dispersive X-ray spectroscopy (EDS) was taken on the SEM. The room-temperature photoluminescence (PL) measurement was carried out on an F−4500 spectrophotometer using the 329 nm excitation line of Xe light.

3 Results and discussion

3.1 ZnSe nanocrystals

The crystal structures of the ZnSe microspheres prepared by using 20 mL 1 mol/L NaOH solution and 10 mL hydrazine hydrate at 180 °C for 4 h were investigated by XRD. Figure 1 shows a typical XRD pattern of ZnSe precursors, in which all the diffraction peaks can be well indexed to cubic ZnSe with lattice constants a=0.567 nm, which is in good agreement with the standard PDF data(37−1463).

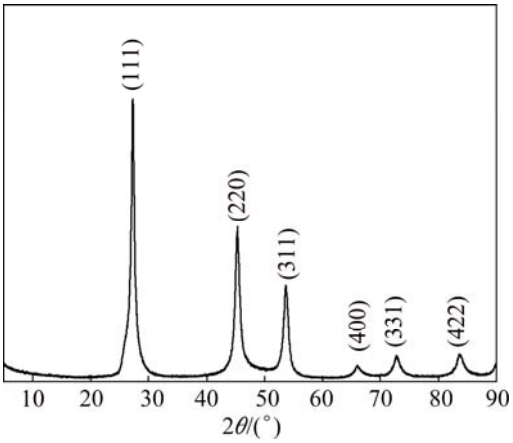

Fig. 1 XRD pattern of as-prepared ZnSe products using 20 mL 1 mol/L NaOH solution and 10 mL hydrazine hydrate at 180 °C for 4 h

The morphology, structure, and size of ZnSe microspheres were characterized with SEM, TEM and HRTEM. As seen in low magnification SEM image (Fig. 2(a)), the diameter of ZnSe spheres is within the range of 1−3 μm. High magnification SEM image (Fig. 2(b)) presents an individual broken ZnSe microsphere, which consists of nanocrystals with average diameter of about 20 nm from inside to outside. SAED pattern of the sphere can be indexed to pure cubic ZnSe (Fig. 2(c)), which suggests that those microspheres are polycrystalline. Further investigations of the ZnSe nanocrystals come from the HRTEM analyses (Fig. 2(d)). The legible crystal lattice reveals the crystal perfection of the ZnSe. Then, the lattice spacing is calculated to be about 0.328 nm, corresponding to the *d*-spacing of (111) crystal plane of the sphalerite ZnSe (theoretically 0.327 nm).

3.2 ZnSe/CdSe core-shell nanocrystals

The ZnSe/CdSe core-shell particles were obtained by combination experiments based on different mole ratios of ZnSe to $Cd(NO_3)_2$. Table 1 lists the amount of reagents in the preparation process. The XRD patterns reveal the crystal structure of the as-prepared products, as shown in Fig. 3. The mixed system can be well indexed to cubic CdSe with lattice constant a=0.605 nm, which is in good agreement with the standard PDF data (65−2891), in addition to cubic ZnSe (Fig. 3(a)). And the main peak height of CdSe increases while the peak height of ZnSe decreases with increasing mole ratio of ZnSe to $Cd(NO_3)_2$. It is worth noting that the diffraction peaks of large angle are significantly shifted to higher angle when they are compared with the standard card, which may be because Zn^{2+} occupies the position of Cd^{2+} in the CdSe lattice. According to Eq. (1), all the products should be CdSe when the mole ratio of ZnSe to $Cd(NO_3)_2$ is 1:1. However, the diffraction peaks of ZnSe do not disappear, which indicates the formation of ZnSe/CdSe nanocomposites.

Figure 3(b) shows that some complex compounds

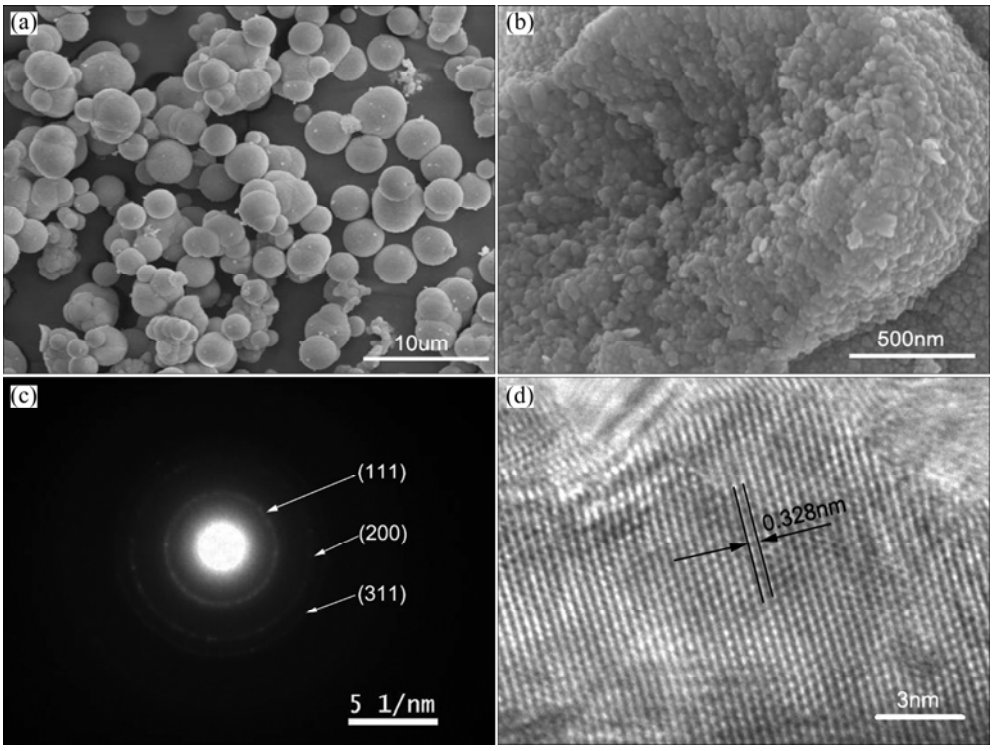

Fig. 2 SEM images (a, b), SAED pattern (c) and HRTEM image (d) of as-prepared ZnSe products using 20 mL 1 mol/L NaOH solution and 10 mL hydrazine hydrate at 180 °C for 4 h

Table 1 Amount of added reagents in preparation process

No.	Amount/mol		Volume/mL	
	ZnSe	$Cd(NO_3)_2$	EDTA	Hydrazine monohydrate
1	0.00100	0.00025	35	5
2	0.00100	0.00050	35	5
3	0.00100	0.00075	35	5
4	0.00100	0.00100	35	5

are produced at larger mole ratios of ZnSe to $Cd(NO_3)_2$ (less than 1:1). The reason is that the dissolution balance of Eq. (2) in the reaction system is destroyed with the increase of the $Cd(NO_3)_2$. Based on Eq. (2), the stable $Cd(OH)_2$ is generated due to its lower value of K_{sp}. Then, $Zn(OH)_2$ cannot be further transformed into $Zn(OH)_4^{2-}$ (Eq. (3)). In another respect, ZnO is obtained with the decrease of pH value on the basis of Eq. (4).

$$Cd^{2+}+2OH^- \rightarrow Cd(OH)_2 \quad (2)$$

$$Zn(OH)_2+2OH^- \rightleftharpoons Zn(OH)_4^{2-} \quad (3)$$

$$Zn(OH)_2 \rightleftharpoons ZnO+H_2O \quad (4)$$

The morphology, microstructure, and size of ZnSe/CdSe core-shell particles were characterized with SEM, TEM and HRTEM, as shown in Fig. 4. Figures 4(a) and (b) show typical low and high magnification SEM images of ZnSe/CdSe core-shell particles, respectively. The ZnSe/CdSe core-shell particles obtained with mole ratio of ZnSe to $Cd(NO_3)_2$

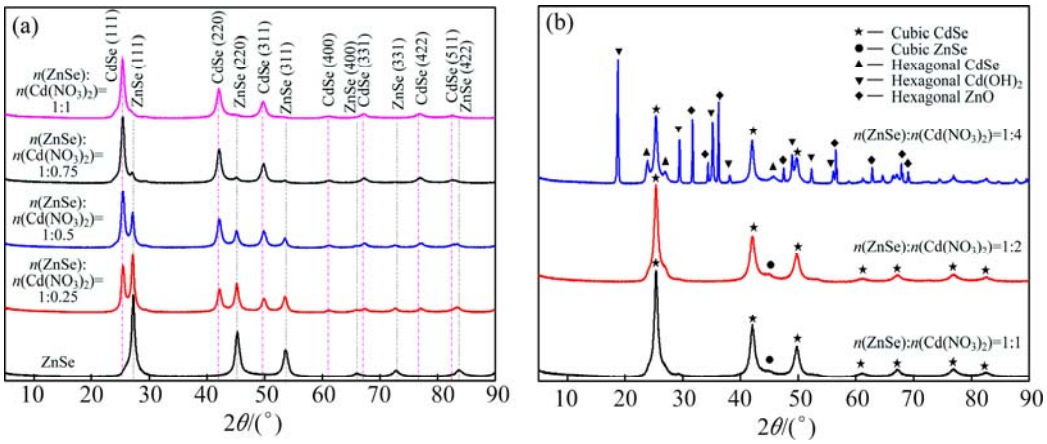

Fig. 3 XRD patterns of products prepared with different mole ratios of ZnSe to $Cd(NO_3)_2$

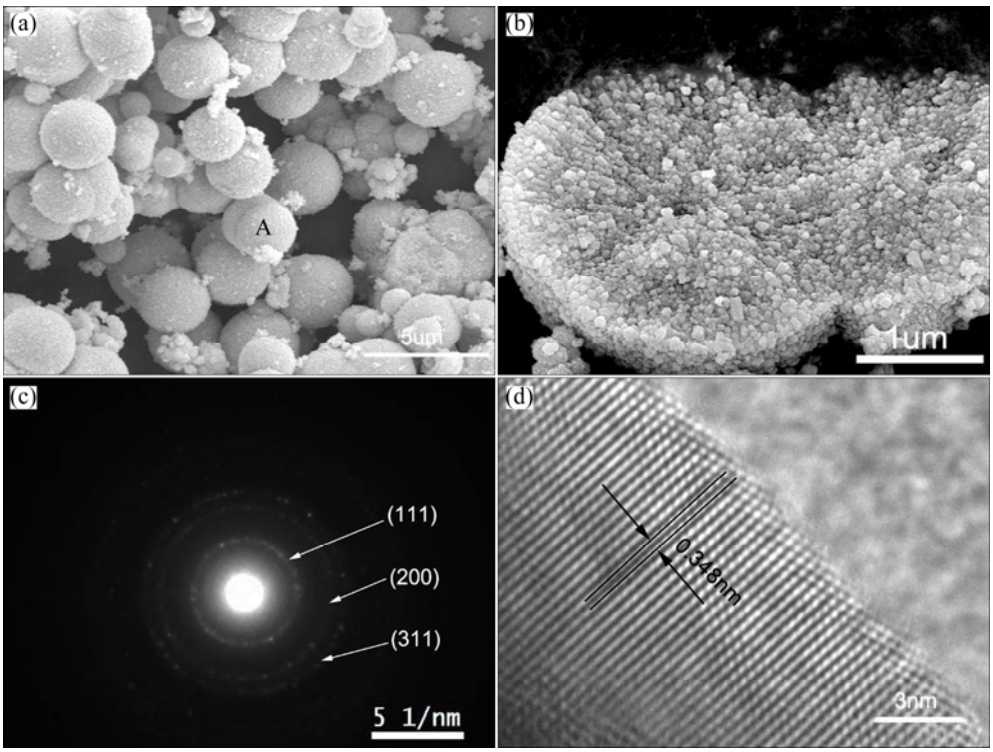

Fig. 4 SEM images (a, b), SAED pattern (c) and HRTEM image (d) of as-prepared ZnSe/CdSe core-shell particles obtained with mole ratio of ZnSe to $Cd(NO_3)_2$ of 1:1

of 1:1 are all solid ball building nano-units of ZnSe and CdSe, of which the average diameter is about 3 μm. The EDS analysis reveals that the products contain Zn, Cd and Se in addition to C (Fig. 5), which is caused by the C substrate, consistent with XRD characterization. SAED pattern of the sphere could be indexed to pure cubic CdSe (Fig. 4(c)), which suggests that those microspheres are polycrystalline. Detailed information regarding to the crystal structure of final products was investigated by HRTEM. Figure 4(d) shows a typical HRTEM image of an individual ZnSe/CdSe core-shell particles. The lattice spacing was calculated to be 0.348 nm, corresponding to the *d*-spacing of (111) crystal plane of the cubic CdSe (theoretically 0.350 nm).

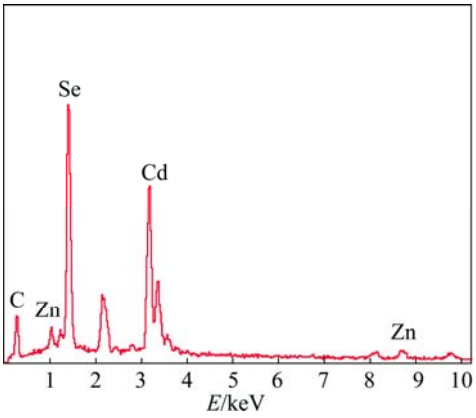

Fig. 5 EDS spectra of particle A in Fig. 4(a)

Figure 6(a) presents the micro-morphology of ZnSe/CdSe core-shell nanocomposites prepared with mole ratio of ZnSe to $Cd(NO_3)_2$ of 1:0.5. Compared with ZnSe/CdSe core-shell particles obtained with mole ratio of ZnSe to $Cd(NO_3)_2$ of 1:1, there are many distinct hollow shells with an average thickness of about 70 nm to be observed (detailed in the inset Fig 6(a)). The broken shell with distinct edges and the fine nano-units are clearly visible in Fig. 6(b). Cd is found in the result of EDS analysis besides Zn and Se (Fig. 7), agreeing with XRD pattern. The products were also studied by using TEM and the result is shown in Fig. 6(c). The small distinct gap, which exists between the ZnSe cores and the initial CdSe shells, is the core-shell structured nature of the as-prepared products. Further HRTEM investigations show that the legible crystal lattice displays crystal perfection (Fig. 6(d)). The calculated lattice spacings (indicated by the arrows) are 0.342 nm and 0.370 nm, which are not in good agreement with the (111) plane of face-centered cubic CdSe (theoretical 0.350 nm). One interpretation for this is that Zn^{2+} replaces the position of Cd^{2+} in the CdSe lattice. The lattice spacing observed (0.342 nm) is between the (111) crystal planes of CdSe and ZnSe (theoretical 0.327 nm), which further confirms the formation of the core-shell structure. In addition, many vacancy defects are formed owing to the Cd^{2+} diffusion during the conversion of ZnSe to ZnSe/CdSe core-shell nanocomposites. So, the calculated lattice spacing (0.370 nm) is larger than that of the (111) plane of face-centered cubic CdSe (theoretical 0.350 nm).

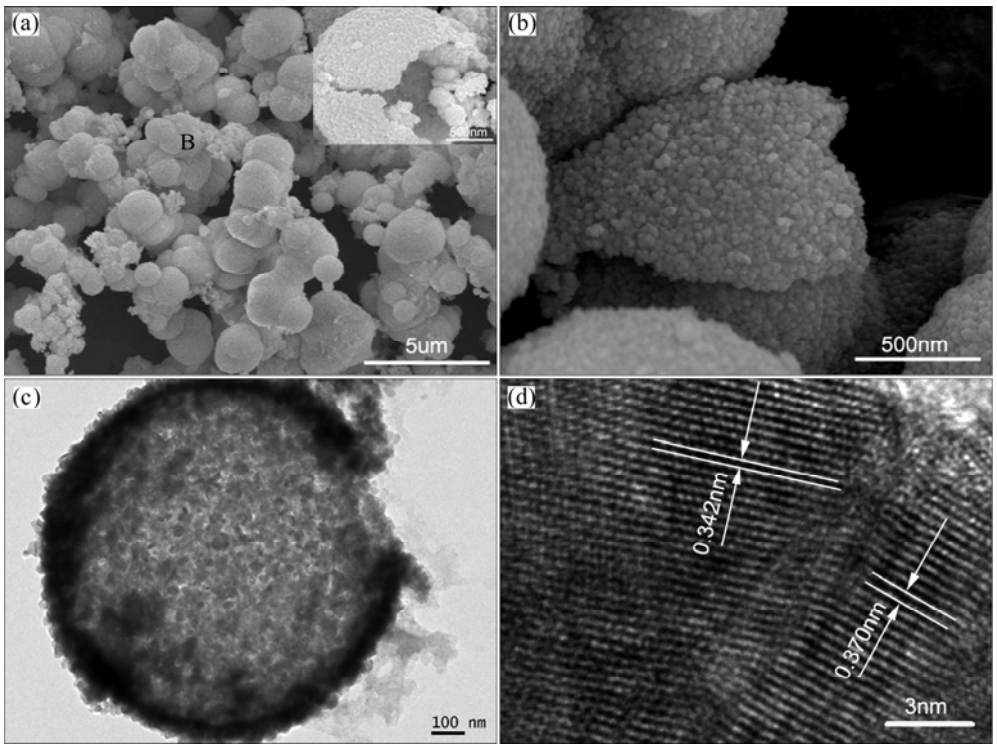

Fig. 6 SEM images (a, b), TEM image (c) and HRTEM image (d) of as-prepared ZnSe/CdSe core-shell particles obtained with mole ratio of ZnSe to $Cd(NO_3)_2$ of 1:0.5 (Inset of (a) is high-magnification SEM images of corresponding product)

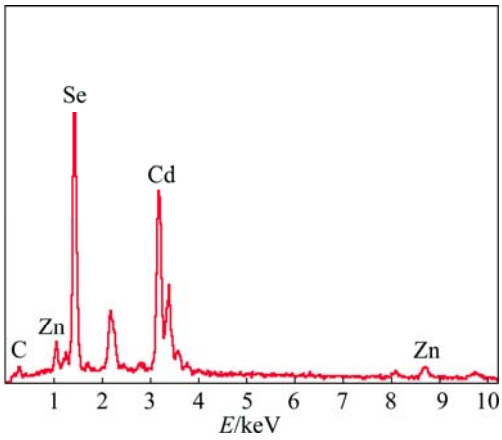

Fig. 7 EDS spectra of particle B in Fig. 6(a)

The influence of the mole ratio of ZnSe to $Cd(NO_3)_2$ on the morphology of the final products was investigated. Figure 8 gives the SEM images of the as-prepared ZnSe/CdSe core-shell particles obtained with mole ratio of ZnSe to $Cd(NO_3)_2$ of 1:0.25 and 1:0.75. Many distinct hollow shells with thicknesses of about 50 nm and 100 nm are obtained (more details in the inset of Figs. 8(a) and (c)). The core-shell structure of the products is clearly observed at high magnifications (Figs. 8(b) and (d)). The thickness of the shell increases with the dose of $Cd(NO_3)_2$ increasing, while the particle size of the building nano-units of ZnSe/CdSe core-shell particles increases (Figs. 8(b) and (d)). According to the above results, we deduce that the core-shell products can be synthesized with the mole ratio of ZnSe to $Cd(NO_3)_2$ more than 1:1.

The room-temperature photoluminescence (PL) experiment was performed to investigate the optical properties of the as-prepared products under the excitation wavelength of 329 nm. Figure 9 presents the PL spectrum of the ZnSe and the as-prepared particles obtained at different mole ratios of ZnSe to $Cd(NO_3)_2$ in the wavelength range of 400−600 nm. The PL spectrum of ZnSe particles presents a broad and well-resolved peak at around 450 nm. The absorption peak shows obvious blue shift relative to the bulk one (460 nm) [18], and a band green emission with peak at 530 nm can be observed. The blue emission originates from the excitonic recombination corresponding to the near-band edge emission of ZnSe, which may be attributed to the quantum-confined effect of the nanocrystals aggregating on the spheres [19]. The green luminescence can be attributed to the recombination of an electron and a photon generated hole caused by surface defects [20]. Compared with ZnSe particles, all of the ZnSe/CdSe core-shell nanocomposites prepared with different mole ratios of ZnSe to $Cd(NO_3)_2$ exhibit the same blue and green emissions. It is also found that mostly the emission peaks of ZnSe/CdSe core-shell nanocomposites are stronger than those of ZnSe particles. However, the emission peaks of the as-prepared particles obtained with molar ratio of ZnSe to $Cd(NO_3)_2$ of 1:1 are weaker than

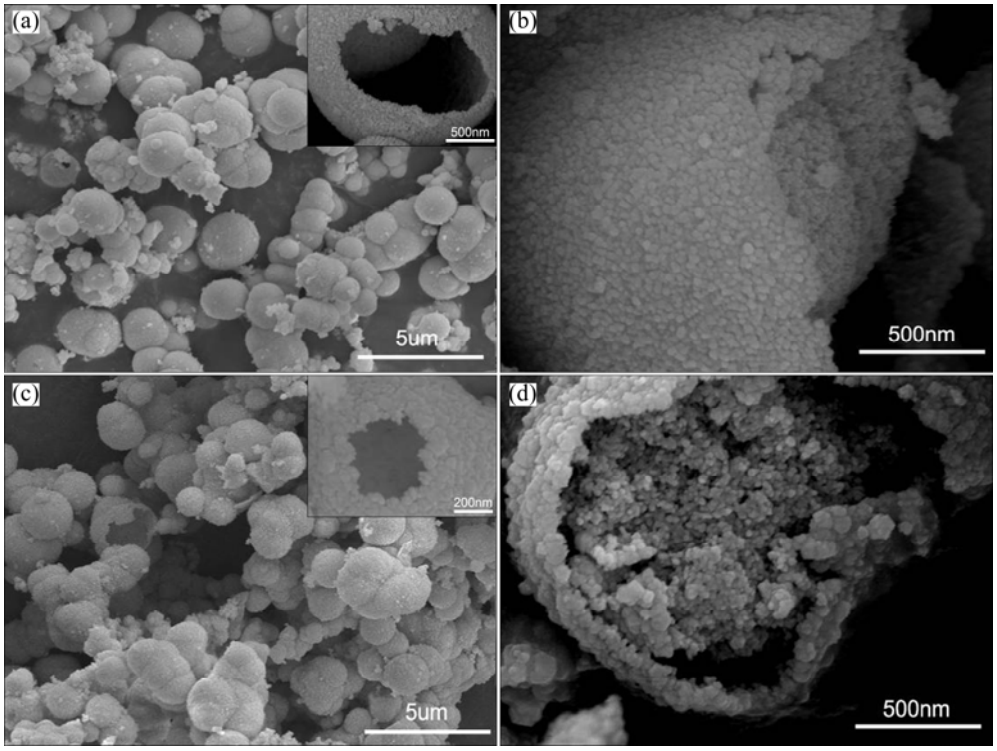

Fig. 8 SEM images of as-prepared ZnSe/CdSe core-shell particles obtained with mole ratio of ZnSe to $Cd(NO_3)_2$ of 1:0.25 (a, b) and 1:0.75 (c, d), respectively (Insets of (a) and (c) are high-magnification SEM images of corresponding products)

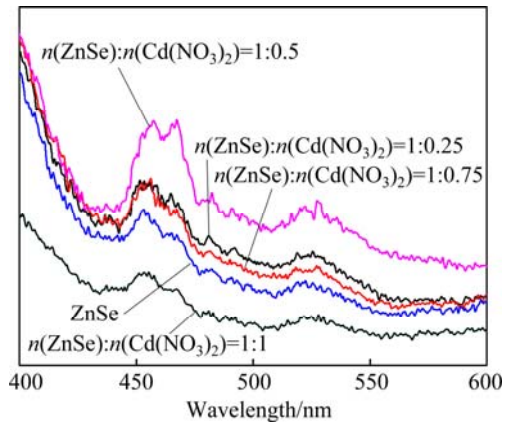

Fig. 9 Photoluminescence (PL) spectra of ZnSe and ZnSe/CdSe core-shell nanocomposites prepared with different mole ratios of ZnSe to $Cd(NO_3)_2$ of 1:0.25, 1:0.5, 1:0.75 and 1:1 under excitation wavelength of 329 nm at room temperature

those of ZnSe particles, in which the emission peaks are not obvious.

The improved PL emission has also been reported in the study of CdS/ZnS wires and CdSe/CdS/ZnCdS/ZnS nanostructures [21]. The portion of CdSe shells closely coating on ZnSe cores provides an efficient passivation of the surface trap states, giving rise to a strongly enhanced fluorescence quantum yield and thus resulting in the obvious enhancement in the ultraviolet emission of ZnSe/CdSe core-shell nanocomposites.

The intrinsic emission (blue emission) peak intensity of core-shell nanocomposites is improved due to CdSe covering the surface of the ZnSe to provide more quantum transition path. Thus, the number of fluorescence photons generated significantly increases to enhance the emission intensity of core-shell nanocomposites material [22]. Meanwhile, many defects and vacancies were generated in the grains as the diffusion of Zn^{2+} and Cd^{2+}, which enhance the non-intrinsic emission (green emission) intensity [17].

The luminous intensity of the ZnSe/CdSe core-shell nanocomposites prepared with mole ratios of ZnSe to $Cd(NO_3)_2$ of 1:0.5 is stronger than those under the mole ratios of 1:0.75 to 1:0.25. When the as-prepared ZnSe/CdSe core-shell particles were obtained with mole ratio of ZnSe to $Cd(NO_3)_2$ of 1:0.25, probably because of many hollow structure (Fig. 8(b)) and insufficient diffusion of Zn^{2+} and Cd^{2+}, the formation of vacancies or defects is not so much and cannot improve the luminous performance significantly. And when the products were obtained with mole ratio of ZnSe to $Cd(NO_3)_2$ of 1:0.75, because of severe diffusion of Zn^{2+} and Cd^{2+}, the shell structure may be more susceptible to breakage and the core-shell structure may be more easily destructed (Fig. 8(d)), which have a negative impact on the performance. If the mole ratio of ZnSe to $Cd(NO_3)_2$ is 1:1, the products which may be very unstable with the core-shell structures or solid ball (Fig. 4(b)) lead to the weakest luminous intensity.

The conversion of solid templates to core-shell or hollow nanostructures is worth exploring. Several formation mechanisms have been proposed to elucidate the process, including the well-known Ostwald ripening [23], classic and newly prevalent Kirkendall effect [24], and in equivalent exchange of metallic atoms regarding the galvanic replacements reaction, and so on [25]. The sketch map of the conversion process is given in Fig. 10. In this work, the diffusion and consumption mechanism of atoms can be utilized to reveal the formation of ZnSe/CdSe core-shell or hollow nanostructures. The solid CdSe microspheres and hollow shell CdSe structure were synthesized by ZnSe microsphere with the dose of $Cd(NO_3)_2$ increasing. Figure 10(a) shows that the core-shell structure transforms into the solid microsphere and hollow shell structure. In the initial stage, ZnSe reacts with Cd^{2+} when it is introduced at certain temperature (140 °C) to produce CdSe, and thus ions exchange happens as Cd^{2+} reacts with Zn^{2+} slowly, dissolved from the surface of ZnSe microspheres to form initial CdSe shells under the driving force caused by the fact that CdSe is more thermodynamically stable due to its lower solubility (Eq. (1)). Small gaps are formed between the ZnSe cores and the initial CdSe shells because the surface of ZnSe gradually evolves into CdSe. The formation mechanism of ZnSe/CdSe core-shell nanocomposites is analyzed in Fig. 10(b). Part of ZnSe in contact with CdSe shells (Fig. 6(d)) stochastically remains and serves as convenient transportation channels, similar to bridges, for Cd^{2+} to reach the reaction interface via surface and bulk diffusion process. Meanwhile, Zn^{2+} continuously diffuses from the inside of ZnSe cores to the outer surface of the CdSe shells. Therefore, many Zn^{2+}, Cd^{2+} and vacancies form in the outer structure of the microspheres. It is easier for Zn^{2+} to penetrate through the CdSe shells due to the smaller size of Zn^{2+}. With the proceeding of the conversion reaction, the CdSe shells become thicker as more and more CdSe nanoparticles pile upon the initial CdSe shells due to the continuous consumption of ZnSe cores and ZnSe/CdSe core-shell nanocomposites are obtained correspondingly. In the reaction systems, both the core-shell structure (Fig. 6(d), Figs. 8(b) and (d)) and the hollow structure (inset of Figs. 8(a) and (c)) can form when the mole ratio of ZnSe to $Cd(NO_3)$ is more than 1:1; and the hollow structure may be evolved from the broken core-shell structure (Fig. 10(b)). However, when the mole ratio is equal to 1:1, the solid ball CdSe structure (Fig. 4(b)) can be obtained.

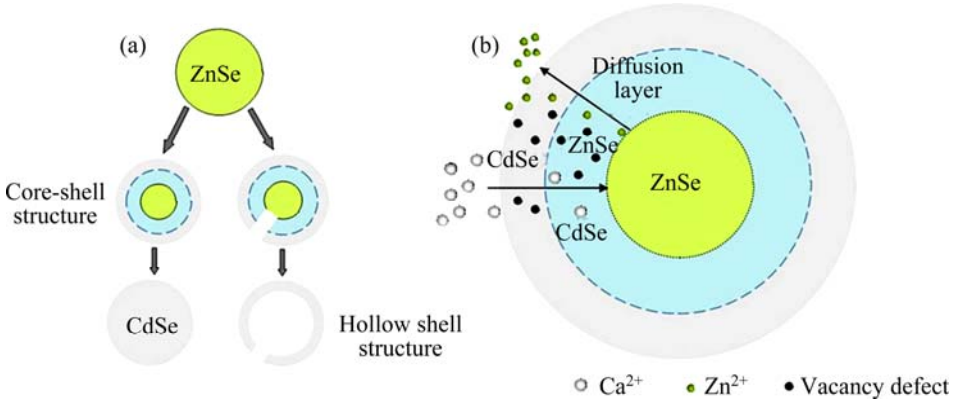

Fig. 10 Schematic illustration of conversion process from ZnSe microspheres to ZnSe/CdSe core-shell or hollow nanostructures (a) and formation mechanism of ZnSe/CdSe core-shell nanocomposites (b)

4 Conclusions

1) When the mole ratio of ZnSe to $Cd(NO_3)_2$ is more than 1, the core-shell structure product can be prepared. When the mole ratio is equal to 1, the product will be ball solid structure.

2) The PL results show that ZnSe/CdSe core-shell structures have high PL emission properties, and the product with mole ratio of 1:0.5 has the best luminescence properties.

3) The luminescence mechanism of product is that ZnSe coated by CdSe can provide more transition path, thus significantly increase the number of fluorescence photons, and enhance the emission properties; while on the other hand, with Zn^{2+} and Cd^{2+} diffusing, a lot of vacancies or interstitial defects form in grain interior, which can enhance extrinsic emission intensity.

Acknowledgments

The authors are grateful to Dr. Sheng-lian YAO for her constructive discussion and useful suggestions.

References

[1] REISS P, CARAYON S, BLEUSE J, PRON A. Low polydispersity core/shell nanocrystals of CdSe/ZnSe and CdSe/ZnSe/ZnS type: Preparation and optical studies [J]. Synthetic Metals, 2003, 139(3): 649−652.

[2] ZHAO Li, YU Jia-guo, CHENG Bei. Preparation and characterization of SiO_2/TiO_2 composite microspheres with microporous SiO_2 core/mesoporous TiO_2 shell [J]. Journal of Solid State Chemistry, 2005, 178(6): 1818−1824.

[3] COE S, WOO W K, BAWENDI M G, BULOVIC V. Electroluminescence from single monolayers of nanocrystals in molecular organic devices [J]. Nature, 2002, 420: 800−803.

[4] GROENEVELD E, WITTEMAN L, LEFFERTS M, KE X X, BALS S, TENDELOO G V, DONEGA C M. Tailoring ZnSe–CdSe colloidal quantum dots via cation exchange: From core/shell to alloy nanocrystals [J]. ACS Nano, 2013, 7(9): 7913−7930.

[5] IVANOV S A, PIRYATINSKI A, NANDA J, TRETIAK S, ZAVADIL K R, WALLACE W O, WERDER D, KLIMOV V I. Type-II core/shell CdS/ZnSe nanocrystals: Synthesis, electronic structures, and spectroscopic properties [J]. Journal of the American Chemical Society, 2007, 129(38): 11708−11719.

[6] TALAPIN D V, KOEPPE R , GÖTZINGER S , KORNOWSKI A, LUPTON J M, ROGACH A L, BENSON O, FELDMANN J, WELLER H. Highly emissive colloidal CdSe/CdS heterostructures of mixed dimensionality [J]. Nano Letter, 2003, 3(12): 1677−1681.

[7] SHEN Xiang, WANG Yan-xin, YANG Xiang, XIA Yong, ZHUANG Jian-feng, TANG Pei-duo. Megahertz magneto-dielectric properties of nanosized NiZnCo ferrite from CTAB-assisted hydrothermal process [J]. Transactions of Nonferrous Metals Society of China, 2009, 19(S3): s1588−s1592.

[8] LAO Jing-yu, WEN Jian-guo, REN Zhi-feng. Hierarchical ZnO nanostructures [J]. Nano Letter, 2002, 2(11): 1287−1291.

[9] JEONG Kang-young, JUNG Hyun-kyung, LEE Hyung-woo. Effective parameters on diameter of carbon nanotubes by plasma enhanced chemical vapor deposition [J]. Transactions of Nonferrous Metals Society of China, 2012, 12(S3): s712−s716.

[10] WANG Li-ping, HUANG Zhu-cheng, ZHANG Ming-yu. Modification of ACFs by chemical vapor deposition and its application for removal of methyl orange from aqueous solution [J]. Transactions of Nonferrous Metals Society of China, 2013, 23(2): 530−537.

[11] CHOI K S, LICHTENEGGER H C, STUCKY G D. Electrochemical synthesis of nanostructured ZnO films utilizing self-assembly of surfactant molecules at solid−liquid interfaces [J]. Journal of the American Chemical Society, 2002, 124(2): 12402−12403.

[12] LIU C H, ZAPIEN J A, YAO Y, MENG X M, LEE C S, FAN S S, LIFSHITZ Y, LEE S T. High-density, ordered ultraviolet light-emitting ZnO nanowire arrays [J]. Advanced Materials, 2003, 15(10): 838−841.

[13] JIAO Yang, YU Da-bin, WANG Zi-rong, TANG Kun, SUN Xiao-quan. Synthesis, nonlinear optical properties and photoluminescence of ZnSe quantum dots in stable solutions [J]. Materials Letters, 2007, 61(7): 1541−1543.

[14] BANDARANAYAKE R J, WEN G W, LIN J Y, JIANG H X, SORENSEN C M. Structural phase behavior in II–VI semiconductor nanoparticles [J]. Applied Physics Letters, 1995, 67: 831−833.

[15] YANG Yang, CHU Ying, ZHANG Yan-ping, YANG Fu-yong, LIU Jing-lin. Polystyrene-ZnO core-shell microspheres and hollow ZnO structures synthesized with the sulfonated polystyrene templates [J]. Journal of Solid State Chemistry, 2006, 179(2): 470−475.

[16] DUAN Yu-lu, YAO Sheng-lian, DAI Cheng, LIU Xiao-he, XU

Guo-fu. Characterization of ZnSe microspheres synthesized under different hydrothermal conditions [J]. Transactions of Nonferrous Metals Society of China, 2014, 24(8): 2588−2597.

[17] PENG Qing, XU Sheng, ZHUANG Zhong-bin, WANG Xun, LI Ya-dong. A general chemical conversion method to various semiconductor hollow structures [J]. Small, 2005, 1(2): 216−221.

[18] HAN Xue, SUN Jing, WANG Hong-li, DU Xi-wen, YANG Jing. Strong green emission from ZnSe–Ag_2Se nanocomposites [J]. Journal of Alloys and Compounds, 2010, 492(1−2): 638−641.

[19] WANG Hong-ni, DU Fang-lin. Hydrothermal synthesis of ZnSe hollow micropheres [J]. Crystal Research and Technology, 2006, 41(4): 323−327.

[20] LIANG J B , LIU J W, XIE Q, BAI S, YU W C , QIAN Y T. Hydrothermal growth and optical properties of doughnut-shaped ZnO microparticles [J]. The Journal of Physical Chemistry B, 2005, 109(19): 9463−9467.

[21] DATTA A, PANDA S K, CHAUDHURI S. Synthesis and optical and electrical properties of CdS/ZnS core/shell nanorods [J]. The Journal of Physical Chemistry C, 2007, 111(46): 17260−17264.

[22] YU Liao, YU Xue-feng, QIU Yong-fu, CHEN Yi-jian, YANG Shi-he. Nonlinear photoluminescence of ZnO/ZnS nanotetrapods [J]. Chemical Physics Letters, 2008, 465(4−6): 272−274.

[23] CHANG Yu, TEO Joong-jiat, ZENG Hua-chun. Formation of colloidal CuO nanocrystallites and their spherical aggregation and reductive transformation to hollow Cu_2O nanospheres [J]. Langmuir, 2005, 21(3): 1074−1079.

[24] FAN H J, GÖSELE U, ZACHARIAS M. Formation of nanotubes and hollow nanoparticles based on kirkendall and diffusion processes: A review [J]. Small, 2007, 3(10): 1660−1671.

[25] AU L, LU Xian-mao, XIA You-nan. A comparative study of galvanic replacement reactions involving Ag nanocubes and $AuCl_2^-$ or $AuCl_4$ [J]. Advanced Materials, 2008, 20(13): 2517−2522.

ZnSe/CdSe 核壳微球的制备与表征

段雨露[1]，周丽旗[1]，徐国富[1,2]，张慧颖[1]，李 旭[1]，刘小鹤[1]

1. 中南大学 材料科学与工程学院，长沙 410083；
2. 中南大学 有色金属材料科学与工程教育部重点实验室，长沙 410083

摘 要：在水热条件下，以水热法合成的 ZnSe 微米球为牺牲模板，成功制备出球形 ZnSe/CdSe 核壳结构纳米复合材料。讨论反应物 ZnSe 和 $Cd(NO_3)_2$ 的不同摩尔比对最终产物形貌和结构的影响，并借助 XRD，SEM，TEM 和 PL 对 ZnSe/CdSe 核壳结构纳米复合材料的性能进行表征。结果表明：当 n(ZnSe):n($Cd(NO_3)_2$ 大于 1:1 时可以制备出核壳结构，n(ZnSe):n($Cd(NO_3)_2$)等于 1 时为实心球结构。PL 光谱表明：ZnSe/CdSe 核壳结构纳米复合材料具有高的 PL 发射强度，且当 n(ZnSe):n($Cd(NO_3)_2$ 为 1:0.5 时发光性能最好。

关键词：水热合成法；核壳纳米复合材料；ZnSe；CdSe；光学性能

(Edited by Yun-bin HE)